Significance of the dynamic modulus of geocell for reinforcing rail embankments

Arghya Chatterjee
Engineering Manager
Stratum Logics
Acheson, Alberta
arghya.chatterjee@stratumlogics.com

Sanat Pokharel
Principal Engineer
Stratum Logics
Acheson, Alberta
sanat.pokharel@stratumlogics.com

Paper prepared for the session SO - Advancements in Testing, Modelling and Innovation for Roadway/Embankment Materials and Geotechnical Engineering
2025 Transportation Association of Canada (TAC) Conference & Exhibition
Québec City, Québec

Acknowledgements

{add any acknowledgements or delete this line and heading above}

Abstract

Railways have been an integral mode of reliable transport for freight and people for centuries. The design of railway embankments is essential in ensuring their stability and performance, particularly their resiliency and safety. Geosynthetics are widely used in rail embankments to optimize embankment thickness and maintain necessary layer separation. Cellular confinement systems (CCS), commonly known as geocells, with their three-dimensional geometry, provide additional confinement effects to increase the modulus of stabilized layers, improve bearing capacity, and reduce the lateral spread of these layers. By confining and stabilizing the ballast, CCS improves load distribution and prevents lateral movement, thereby reducing track settlement and lateral deformation over time. CCS also helps to reduce embankment thickness, lowering material costs while enhancing track performance under heavy loads and high-speed trains.

Another aspect that has recently garnered attention among engineers is the vibration attenuation benefits provided by CCS. In railway operations, one challenge that requires attention during track maintenance is the fouling of ballast and contamination of sub-ballast, which occurs due to particle

abrasion and the migration of fines. While a separation geotextile layer can nearly eliminate the vertical migration of fines, lateral migration intensifies with the lateral spreading and vibration from a passing locomotive load. Vibration plays a crucial role in the development and migration of fines. CCS vibration attenuation has been shown to reduce the time-dependent change in particle distribution within the embankment.

The performance of any reinforcement depends on its material properties. Soil reinforcements are typically made of plastic materials with a viscoelastic character. Viscoelastic materials accumulate strain even when the load is within the elastic limit. As strain increases, the modulus of the material decreases, leading to a quicker accumulation of higher strain. This effectively reduces the stabilization effect, resulting in increased maintenance costs. For design engineers, it is important to understand and correlate the material index properties with the performance life of an embankment. The current paper studies each of the mechanisms of CCS and links them to fundamental material properties. The dynamic modulus and rate of cumulative strain accumulation play a vital role in overall design performance. The concept was implemented while designing a short span of the Big Sky Rail track at Eston and Pasqua loop in Saskatchewan, Canada, in 2019. The four-year visual observation and subsequent maintenance cycles validated the design considerations.

Introduction

The increasing demand for resilient and cost-effective railway infrastructure, especially in regions with challenging geotechnical conditions such as soft soils (Nimbalkar et al., 2020[1]), permafrost (Pokharel and Breault, 2020[2]), has driven significant interest in innovative ground improvement techniques. Among the solutions explored, Cellular Confinement Systems (CCS), also known as geocells, have emerged as a proven and versatile method for reinforcing weak subgrades (Pokharel, 2010[3]), reducing track deformation (Chatterjee et al., 2020[3]), and enhancing long-term performance under repeated dynamic loading conditions (Hegde et al., 2018[5]; Mehrjardi et al. 2012[6]). As detailed in the works of Chatterjee et al., (2025)[7], geocells offer a combination of confinement, energy dissipation, and stiffness improvement, making them highly suited for modern railway applications where high-frequency and heavy loads are the norm. Traditionally, rail embankments relied on thick granular layers to distribute loads and maintain track geometry. However, such designs become inefficient and costly in areas with soft ground or limited material availability (Chatterjee et al., 2024[8]). Geocells, with their three-dimensional honeycomb-like geometry, create a cellular confinement effect that significantly increases the modulus of the stabilized soil layers, thereby reducing the required structural thickness (Chatterjee et al., 2023[4]; Chatterjee et al., 2024[9]; Nimbalkar et al., 2020[1]) and associated costs (Dagenais et al., 2024[10]; Chatterjee et al., 2024[11]). Research has shown that geocells not only increase the bearing capacity of the subgrade but also improve load distribution (Pokharel, 2010[3]) and reduce lateral spreading of the embankment layers (Chatterjee et al., 2024[9]; Pokharel and Breault, 2020[2]). This improved lateral restraint directly translates into reduced long-term deformation under cyclic train loads, minimizing maintenance and extending the design life of rail infrastructure.

Another emerging area of interest among researchers working on geocell technology is its role in attenuating vibrations (Hegde et al., 2018[5], Mehrjardi et al., 2012[6], Amiri et al., 2023[12]), particularly important in railway environments (Nimbalkar et al., 2020[1]). In railways, locomotive-induced vibrations can accelerate ballast degradation, lead to differential settlements, and contribute to the fouling of ballast layers, wherein fine particles infiltrate and clog the voids between ballast stones. This not only reduces the drainage capacity but also compromises the load-bearing efficiency of the track system. Thus,

increasing the maintenance frequency and cost. Although geotextiles are commonly used as a separation layer, to prevent vertical migration of fines or for wicking action (Camila, 2021[13]), lateral migration due to vibration and dynamic loading remains a persistent challenge. This becomes a bigger issue in regions where track maintenance cycles are less frequent or cost-prohibitive due to operational freeze or remote locations. CCS has shown promising results in vibration attenuation, as supported by some experimental and field studies (Hegde et al., 2018[5]; Mehrjardi et al., 2012[6]). The confined system damps dynamic loads and retards the relative particle movement within the embankment layers. By limiting the vibration-induced movement of particles, geocells help stabilize the internal structure of the track, thereby extending the intervals between necessary maintenance operations and improving ride quality.

The lack of an accepted analytical framework to directly link CCS material properties, particularly the dynamic modulus and viscoelastic strain behaviour, with the embankment performance leaves current design practices uncertain, making it either conservative or exposed to unforeseen failures. Attempts to model CCS behaviour through mechanisms such as beam or slab effect (Pokharel, 2010[3]), equivalent layer stiffness (Leshchinsky and Ling, 2013[17]), and interface shear strength (Mehrjardi and Motarjemi, 2018[18]) offer valuable insights but fall short of capturing the full scope of viscoelastic material-structure interaction under dynamic loading.

The current study attempts to theoretically establish the importance of dynamic modulus and how it is related to the performance of CCS-stabilized rail embankment (stress redistribution and damping performance) over time. This involves decoupling the individual mechanisms of reinforcement, such as lateral restraint, vibration attenuation, and layer stiffness improvement, and correlating each to fundamental material index properties. This approach enables a more rational design methodology, where geocell (CCS) selection is informed by measurable, material-specific parameters that change over time rather than generalized assumptions.

The practical implications of this research were demonstrated in the design and construction of a short section of the Big Sky Rail track in Eston, Saskatchewan, in 2019 and in Pasqua, Saskatchewan, Canada, in 2022. This site was selected for its soft subgrade and exposure to dynamic loading conditions typical of heavy freight traffic. The geocell used in the project was chosen based on its high dynamic modulus and high tensile strength, which were necessary to meet the minimum performance expectations over the design life. Over the years of the observation period, visual inspections and maintenance records validated the performance assumptions, showing minimal settlement, reduced fines migration, and extended maintenance intervals (Palese, 2018[33]).

CCS viscoelastic model

All polymers exhibit viscoelastic character because of their molecular structural arrangement (Dunn, 2019)[19]. Commonly used polymers for CCS are High Density Polyethylene (HDPE) and Novel Polymeric Alloy (NPA). These materials have a working range of temperature which matches well for outdoor applications, providing the necessary combination of strength and flexibility. Outside the range of working temperature, viscoelastic materials behave as glass (at low temperatures) or as a non-strength carrying fluid (at high temperatures, even below the melting point). Viscoelastic material can be visualized as a combination of elastic fibres connected by viscous fluid (Figure 1a). As stress is applied, both the elastic fibre and the viscous fluid attain strain. The recovery of that strain within the elastic fibre is instantaneous,

as long as the applied stress is within elastic limits. Meanwhile, the viscous part behaves passively and recovers mostly with a lag (Figure 1b), leading to residual strain even when the stress is removed. This response lag from the viscous part of the material is often used to dissipate large energy in seismic dampers. Additionally, the persistent presence of stress over time leads to strain accumulation from stress relaxation. This cumulative effect takes the viscous part to a higher state of strain where the viscous character dominates over the elastic. This is known as creep-relaxation. CCS material being viscoelastic in nature, considering only the static modulus (like Young's modulus or Secant's modulus) is not ideal to assess its performance over time. For static modulus consideration, one of the fundamental requirements is that the material must not attain any plastic strain while the load is within the elastic limit. Attaining micro-plastic strain at early stages of low stress (Dunn, 2019[19]) brings non-linearity within the stress-strain curve. Thus, making it difficult to agree upon one stiffness value. Also, based on the state of strain, the viscous connection between the elastic fibres shifts, leading to less stress being shared by some elastic fibres. This leads to a loss of modulus even before the material has yielded. This makes knowledge of the material modulus at different states of strain very important for a reliable load-bearing design. One of the universally accepted methods for testing the modulus of the material at elevated strains is called Dynamic Modulus Analysis (DMA). In DMA, instead of applying the quasistatic stress to attain different strains and then measure the modulus over a long time, an accelerated approach with temperature is recommended by ASTM (D7361-07, 2018[32]) standards. The importance of dynamic modulus for CCS design is recognized in ASTM D8269[31] and ISO/TD 18228-5:2025[28]. To attain a higher state of strain, the temperature of the strip material is raised. For each temperature, the modulus is measured. Then, by applying mathematical calibrations, the complete curve of material modulus across the applicable range of strains is plotted. For more dynamic conditions, particularly those involving frequent load reversals, Dynamic Mechanical Analysis (DMA) serves as a versatile and accurate tool. DMA enables the measurement of the material's response under varying frequencies of stress, providing a more detailed understanding of the material's behaviour under complex loading conditions.

This modulus reduction with time and strain accumulation is particularly critical in rail applications where the CCS is subjected to many load cycles over its service life. As strain increases, the effective modulus of the geocell decreases, leading to progressive weakening of the confinement effect. This, in turn, can result in accelerated track deformations and ultimately, higher maintenance costs. The challenge for engineers, therefore, is not just to select a geocell based on its initial tensile strength or elastic modulus, but to understand how its dynamic behaviour will evolve under operational loading conditions.

Damping with viscous material

From DMA, both the dynamic elastic modulus (also known as storage modulus) and the dynamic viscous modulus (also known as loss modulus) are obtained (Equation 1, Equation 2). The ratio of these two moduli represents the lag (Equation 3) in the plastic response. In an ideal situation, a higher elastic modulus and a lower viscous modulus are preferred. The larger the gap, the greater the damping capability. Novel Polymeric Alloy (NPA) material, having a much higher dynamic elastic modulus at higher temperatures and being less prone to creep, shows a significantly higher damping capability. In a lab experiment, Hegde et al. (2018)[5] could achieve around 163% damping using NPA-CCS, while Mehrjardi et al. (2012)[6] saw around 35% with HDPE. Though the test setup was different, it is not fair to compare the exact numbers, even though the results align well with theoretical expectations, with changing the material. For a reinforcing material engineered for railways or similar soil stabilization applications under dynamic loads, the focus is always to have a higher dynamic elastic modulus and a higher gap between

the dynamic elastic and the viscous modulus. This leads to stronger performance over a longer time and a higher damping ratio.

In an ideal elastic material, there is no phase lag within the response, and similarly, for an ideal viscous material, the phase lag is ninety degrees (Figure 1b). For a viscoelastic material, the phase lag is somewhere in between. It must be noted that the loss modulus is not entirely plastic; it recovers over time. Theoretically, given an infinite amount of time, it is expected to recover fully. However, from a practical standpoint, most of the stress is released with time while some relaxes as creep. For any repeated loading, the unrecovered part is larger as there is the possibility of another round of load even before the material has relaxed enough. It is even worse in a soil stabilization application as expansion of the CCS pockets leaves an opportunity for the particles within the pocket to move into a new state of equilibrium, making even the elastic recovery difficult.

$$E' = E^* \cos(\varphi) \tag{1}$$

$$E'' = E^* \sin(\varphi) \tag{2}$$

$$\tan(\varphi) = \frac{E''}{E'} \tag{3}$$

where, E^* is the dynamic modulus, E' is the dynamic elastic modulus (storage modulus), E'' is the dynamic viscous modulus (loss modulus) and $\tan(\varphi)$ is the phase shift.

Typical model of a viscoelastic material

A classical representation of a viscoelastic material is the modified Maxwell model, where the dynamic elastic modulus and the dynamic viscous modulus are in parallel. Also, the non-recovered strain is represented as a dashpot member, which is in series with the dynamic viscous modulus. This model (Figure 2) has been successfully used by others in modelling the viscoelastic nature of polymers (Findley et al., 1977[20]; Wineman, 2009[21]; Banks et al. 2011[22]; Lakes, 2009[24]; Riande et al., 1999[25]). One of the limitations of this model is that the loading is considered as a step function, implying that the rate of loading is infinite (extremely fast). This can be true for a fast-moving locomotive, but for most general applications, using this model will miss the creep that can happen while the material is getting loaded. Some complex models talk about this correction (Lin et al., 2022[23]). However, owing to the speed of locomotives and typical lengths of locomotives, the time required for the CCS to get loaded from the state of zero stress, as compared to the time for which it stays loaded, is small. This makes the relative loading rate fast enough to consider the complex model correction from Lin et al. (2022)[23] negligible. This also keeps the model simple for understanding and with insignificant error.

$$\varepsilon_{creet}(t) = \frac{\sigma_0}{E'}\left(1 - \frac{E''}{E'+E''}\, e^{-t/\tau_c}\right) \tag{4}$$

where,

$$\tau_c = \eta \frac{(E'+E'')}{E'*E''} \tag{5}$$

where, η is the CCS material viscosity and *t* is the time exposure of the load.

Figure 1a. Schematic for a viscoelastic material

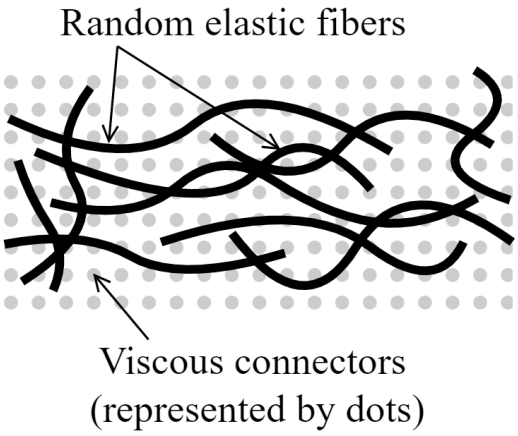

Figure 1b. The phase lag between elastic and viscous response in a viscoelastic material

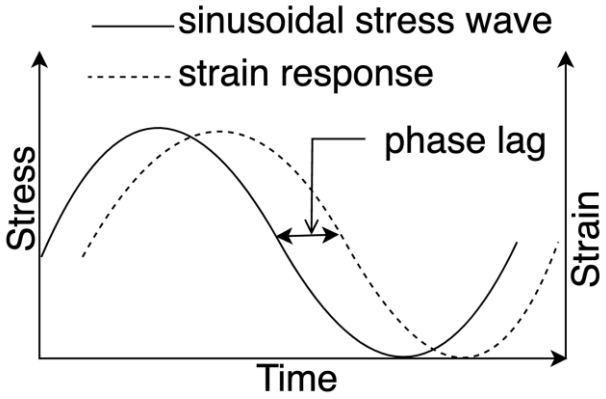

Figure 2. Schematic representation of the viscoelastic model for the CCS

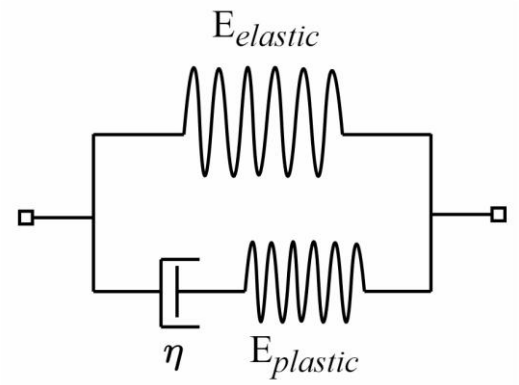

Understanding the load

In railway applications, the dynamically amplified wheel load passes through the track to the ties and then loads the ballast. Owing to the risk of damaging CCS while maintaining ballast, placing CCS within the ballast is not recommended (Pokharel and Breault, 2020[2]). So, the CCS is either placed at the top of the sub-ballast layer to provide some confinement to the ballast along with distributing the load over a wider area or placed on top of the subgrade for the slab effect, holding the embankment on top of weak soil. The advantage of having the right selection of reinforcement (Chatterjee et al., 2023[4]) can not only stabilize the embankment with a significant maintenance cost reduction but also reduce the effective dynamic loads (Chatterjee et al., 2024[9]). In all cases, the geometry of the CCS mustn't change with time over several load cycles to maintain the necessary confinement and load distribution. An increased pocket size leads to a loss of layer modulus, making the slab effect ineffective. This reduces the reinforcement efficiency and thus, a shortened designed life. Chatterjee et al. (2025)[7] have shown that high dynamic modulus CCS is an excellent solution for rail track rehabilitation. No matter where the CCS is placed, the effective forces come to the reinforcing material as tension (either hoop tension or tension from flexure).

Figure 3 shows how the CCS pocket is experiencing the lateral load with its confining ability. For the current hypothetical case, consider Copper E80 loading as per the AREMA standards (Manual for Railway Engineering, 2019[26]). If CCS is placed right under the ballast, with a 250mm thick ballast layer, then the overlap of loading on CCS is from at least three ties (assuming standard one-foot tie spacing). If the CCS is placed at subgrade level, the overlap is five or more, depending on the sub-ballast thickness. The vertical pressure is distributed between vertical deflection and lateral confinement. If a well-prepared sub-grade is assumed, then most of the load is distributed laterally (Figure 3). The CCS pocket right under the load has the maximum vertical stress, and the stress reduces exponentially in the next pocket and onwards (Emersleben et al., 2009[27]). It is the lateral coefficient of the average vertical stress difference between two adjacent CCS pockets that develops the tension on the CCS wall (Figure 4a). If a pocket is divided into four influence zones responsible for the tensile stress on the CCS walls, then the effective pressure on each wall can be calculated. It must be noted that unless the CCS pocket is directly under the load, while two of the influence areas are developing tension, the other two are in compression (Figure 4b). As the wheel load passes, it is this tension that acts on the viscoelastic modelled representative (Figure 2) of the CCS material. In theory, the stress is distributed amongst the elastic and the viscous modulus, leading to viscous strain. A part of this viscous strain has a cumulative effect, leading to a higher state of strain for the reinforcing material.

Figure 3. The dynamic load as experienced by CCS within rail embankments

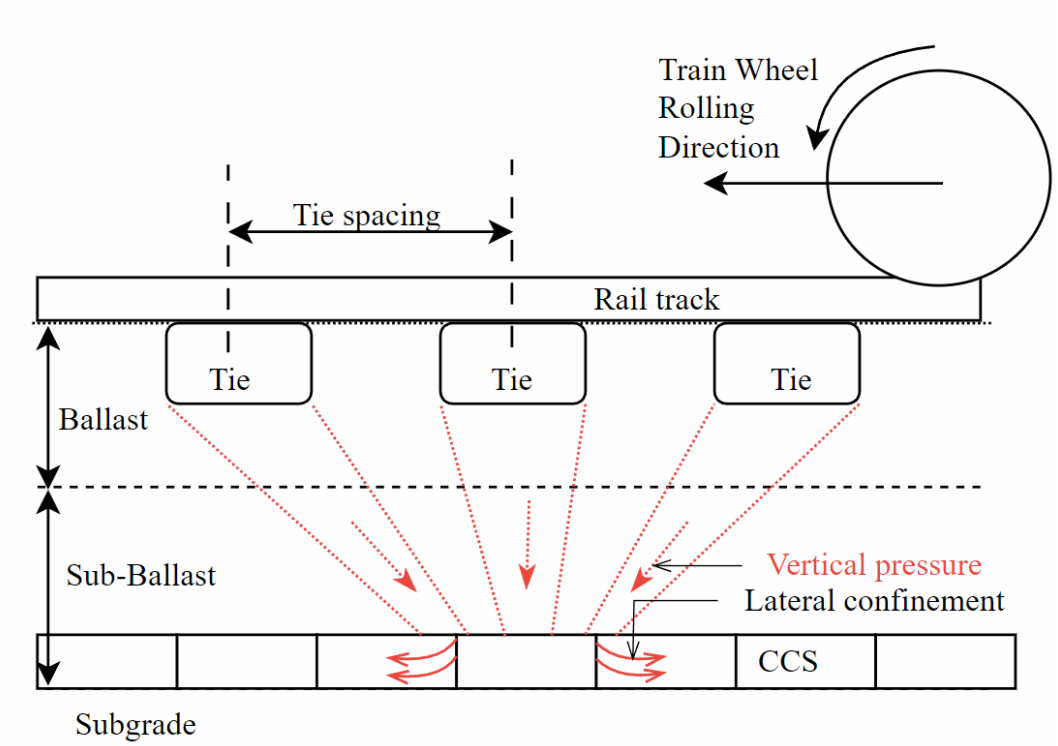

Table 1 represents the hypothetical design where the CCS is placed right below the ballast. The overall design has only one layer of CCS along with a layer of woven textile below. The reason for considering the textile is to consider layer separation and to complete the CCS pocket geometry for lateral and vertical confinement. The ideal reinforcement is chosen based on recommendations in Chatterjee et al. (2023)[4]. The strength reduction from freeze-thaw, the presence of water, and viscous strain from slow loading are not considered here. Though these mechanisms reduce effective design life but they are typically

insignificant in most project scenarios. Typically, the International Standards Organization guides that in soil-stabilization applications (ISO/TD 18228-5:2025[28]), the strain limit needs to be 2%. If the design life needs to be increased, then CCS needs to be placed at a lower depth, where the effective tensile stress on the CCS wall is lower. However, that reduces the efficiency of the reinforcement design as well. Thus, an optimal design must consider the balance between selection of CCS material, CCS geometry, expected design life and best placement location to meet the necessary design life. The viscosity of the CCS material was taken as 400MPa at 120 ^{0}C (as per the supplier's safety data sheet for NPA-CCS). However, polymers at outdoor working temperatures usually have a viscosity range from 1MPa to 1GPa. The influence of viscosity change, within the discussed range, is insignificant in the model (Figure 2).

Table 1. Hypothetical design of the design life of stabilized rail embankment based on CCS material properties

Load	Cooper E80
Maximum Velocity	15 miles/hour
Car length	150 cars (@4axle/car)
Carry load	125 metric tons/car
Car wheel diameter	0.97m
Dynamic load factor (after reduction from CCS, as per Chatterjee et al. 2024)	1.26
Tie detail	7" thick x 9" wide and 8.5' long
Tie material	Wood
Tie spacing (c/c)	21"
CCS Type	NPA-CCS Type D
CCS pocket size	210mm x 245mm x 150mm high
CCS Tensile strength	22kN/m
DMA (Elastic) [from Chatterjee et al. 2025]	@30 0C, E'=2246 MPa @45 0C, E'=1365 MPa @60 0C, E'=865 MPa @75 0C, E'=547 MPa
Limiting Strain [from ISO/TD 18228-5:2025[28]]	2%
Number of passes allowable	670
Considering 1 car every alternate day and no operation for 1 month/year, design life of reinforcement	4 years

Figure 4a. Stress distribution within CCS pockets

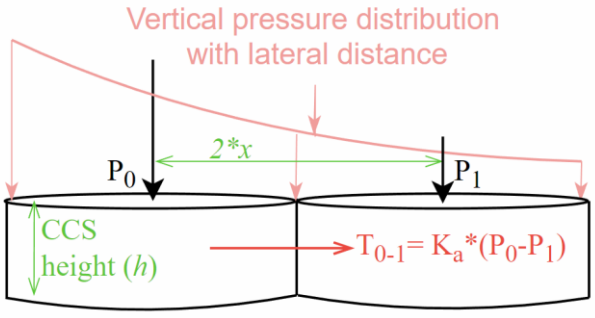

Figure 4b. Tension and compression walls within CCS under stress

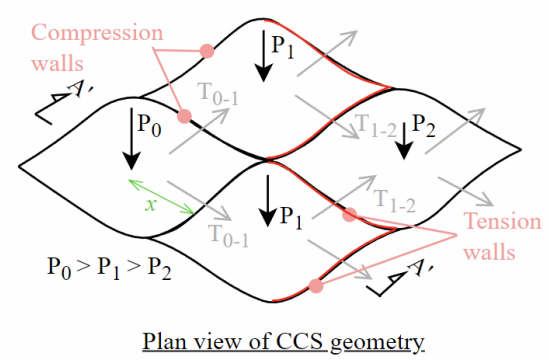

Design implementation

The concept of viscoelastic material and dynamic modulus was applied towards designing two full-scale projects. Owing to the contractual dynamics, instrumentation for observation was not possible. However, the sites were monitored visually and a routine survey at one of the sites was carried out. Chatterjee et al. (2024)[29] presented the details on the design and implementation of the Pasqua project. A similar methodology was implemented for the design of the Easton Rail. Both these designs involved building the embankment on soft ground (Figure 6a, Figure 6b, Figure 11 and Figure 13), demanding the bottom layer of CCS be right on top of the subgrade to reduce the bearing dependency on sub-grade strength. The upper layer was added to spread the load over a wider area and also to provide the necessary confinement. At Easton there was stiffness jump from natural subgrade to concrete, and that increased the effective risk of track deformation (Figure 5 and Figure 9). Figure 7 shows the typical cross-section for both project sites. Also, a two-layer design was chosen to minimize the lateral spread of ballast and sub-ballast with redistribution of forces and damping the locomotive vibrations. Thus reduce, if not eliminate, maintenance and operational interruptions. Local sand with less than 15% fines was used as sub-ballast, and this was acceptable owing to the virtual bulk properties that could be added to the stabilized layer using the high dynamic modulus of NPA-CCS. Identical calculations were carried out as part of the design, as shown in Table 1, to assess the design performance life. The primary target was to completely eliminate operational hindrance from maintenance for at least the initial three years.

At Easton, the groundwater table in summer was within 150mm of the subgrade elevation (somewhat visible on Figure 6a). The section that demanded rehabilitation had a stiffness jump as the track transitioned from concrete to prepared subgrade (Figure 5). For Pasqua, the geometric deformation shown on the track (Figure 10) was from uneven stiffness developed within the embankment from injecting resin foam to raise the track to the design elevation. Based on the design, the amount of stress that was transmitted to the subgrade in Pasqua and Easton were 8.5% and 9.2% respectively.

In both projects, the dynamic modulus was used to understand the degradation of the reinforcing material properties. Based on the number of loaded and unloaded passes per day, design life and expected maintenance cycles were computed. Easton was constructed in September 2019, while a relatively bigger scope with the Pasqua loop (Figure 12) track was constructed in June 2022. One of the additional considerations for loop track is overloading the inner track with slower locomotive movement, as stated by Chatterjee et al. (2024)[9]. The possible range of velocities was tested to calculate the optimum load and

relevant CCS material modulus loss over each train pass. Figure 8 and Figure 9 show the bottom and the top layer of CCS being built at Easton, respectively. Similarly, Figure 14 and Figure 15 show the bottom (with NPA-CCS Type C) and top layers (NPA-CCS-Type D) for the Pasqua loop, respectively. In design, based on the applicable member stresses, the number of allowable passes is checked for both layers of both projects, similar to the calculations shown in Table 1. The tracks have been under critical observation since it's construction.

Figure 5. At Easton rail track issue from the stiffness transition and lateral spreading of ballast

Figure 6a. At Easton, the exposed subgrade has with water table close to the surface and the presence of concrete crossing

Figure 6b. Fouling of ballast and ties, getting pushed into the embankment from the track vibration (at Easton)

Figure 7. Typical cross-section with CCS

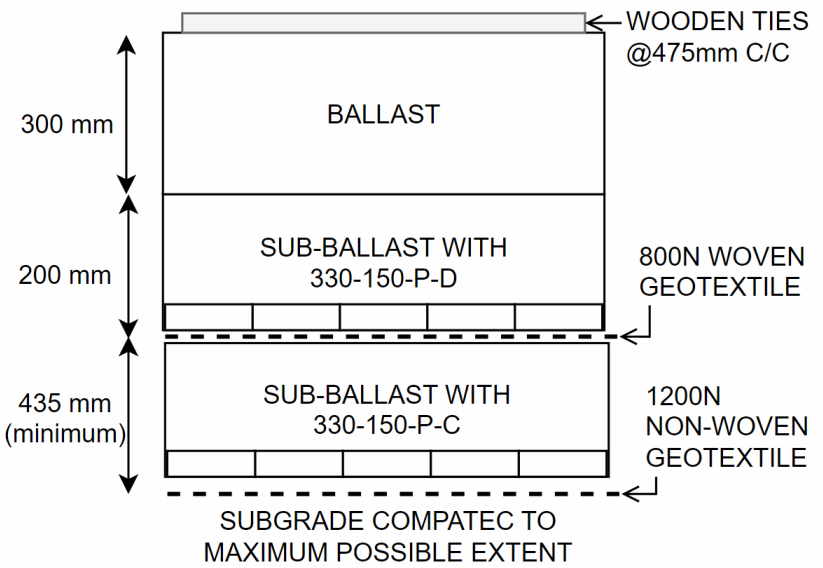

Figure 8. Bottom layer of NPA-CCS (Type C) at Easton

Figure 9. The top layer of NPA-CCS (Type D) smoothening the stiffness transition at Easton

Figure 10. At Pasqua, the non-uniform stiffness created by resin foam injection

Figure 11. At Pasqua, the exposed soft subgrade

Figure 12. The Pasqua loop

Figure 13. The prepared subgrade at the Pasqua loop

Figure 14. Bottom layer of NPA-CCS (Type C) at Pasqua loop

Figure 15. Top layer of NPA-CCS at Pasqua

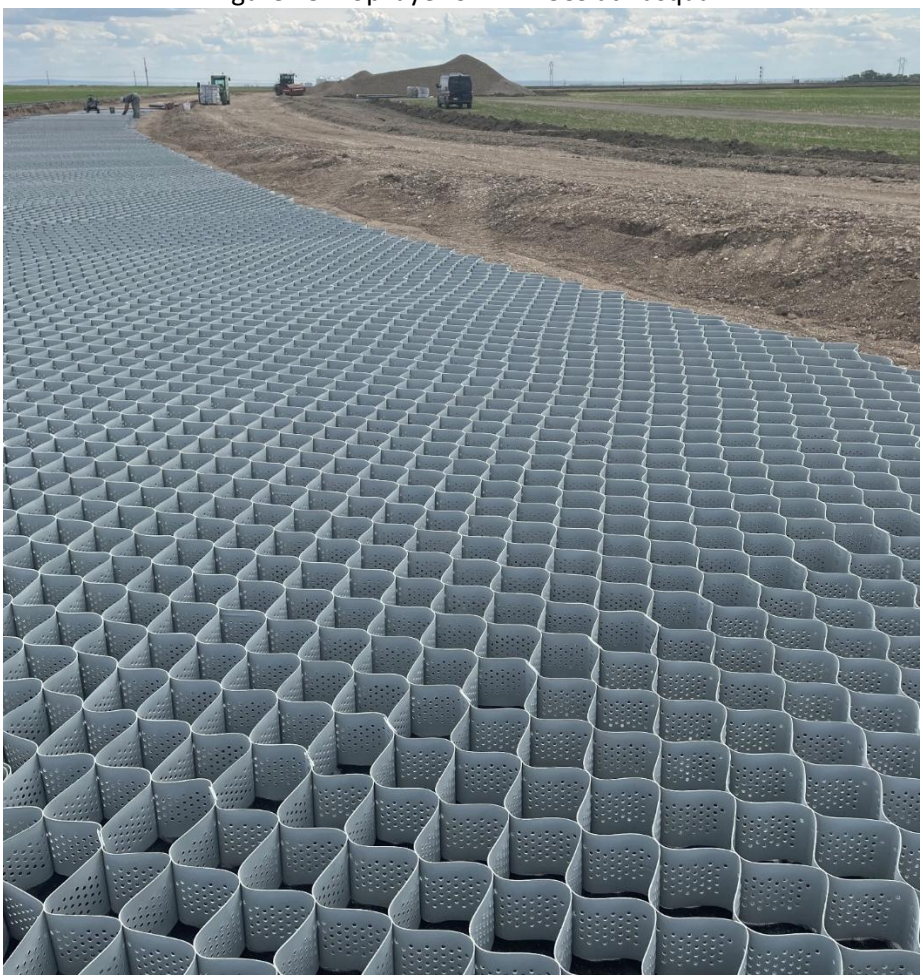

Results and Discussions

The angle derived from the phase lag is an indirect indicator of the possible damping. If CCS is fully elastic, then the angle would be $\varphi = 0^0$, and if it were viscous only, with no elastic component, then the angle would be $\varphi = 90^0$. For the selected CCS, the angle varies between $\varphi = 14^0$ to 18.5^0 (Figure 17). This shows that the CCS material selected is almost 80% elastic (= [90^0-phase angle/90^0] %). A higher angle will increase the damping possibility, but at the same time, it will be a compromise on the initial stress and long-term strengths. So, a good design must select materials based on the site-specific demand. The material damping is based on the phase lag, which, based on Figure 17, is almost independent of how much stress is acting on the CCS and at what state of strain the CCS is present. However, this stress dependency on damping is dependent on the selected CCS material. If HDPE is selected for CCS material, using the properties stated by Mohagheghian et al. (2015)[30] the percentage elastic (% offset of phase angle from 90^0) based on the modulus ratio starts around 80% at 30 ^{0}C (lower state of strain). However, at elevated temperatures (higher state of strain at around 60 ^{0}C), the ratio of elastic falls to less than 40% ($\varphi > 61^0$). This may seem attractive from a damping perspective. However, if the support strength is lost, then no use in having high damping. Also, the damping advantage happens within the stabilized layer and anything under it. If the CCS is placed deep enough to minimize the acting load, the unstabilized ballast and sub-ballast materials will experience the same fouling and abrasion effects from the dynamic vibrations of passing locomotives as they would in an unreinforced condition. Depending on the applied load, the subgrade conditions and the elevation at which the CCS is installed, the acting stresses on CCS walls can be determined. Once the stresses are known, the required material modulus can be chosen based on the target number of passes, based on Figure 18. If the range of material modulus is outside the market availability, then the placement depth of CCS needs to be compromised to achieve the necessary number of passes.

Despite widespread recognition of geocell benefits in railways (Indraratna et al., 2015[14]; Nimbalkar et al., 2012[15]), there remains a critical gap in understanding and quantitatively correlating the material index properties that are necessary to maintain the minimum serviceability requirements of the structural layers through its design life. Much of the current design practice still does not quantify how specific material parameters, such as the dynamic modulus, influence the field performance of CCS-reinforced rail embankments. Typically, the analytical models focus on idealized or simplified representations of load transfer (Kief et al., 2011[16]; Pokharel, 2010[3]), often treating the geocell as an elastic support layer, without accounting for time-dependent or strain-rate-dependent material strength reduction. However, the performance of CCS is intrinsically linked to the material properties of the geocell strips, particularly their viscoelastic strength loss over time. Unlike elastic-plastic materials that behave predictably within a linear elastic range, viscoelastic polymers accumulate strain over time, even under sub-yield stress conditions. This means that a geocell can undergo internal rearrangements and molecular-level deformations. Thus, resulting in plastic strain accumulation from stress relaxation, even when it appears to remain within safe operational limits. The dynamic modulus, which represents the stiffness of a material under cyclic loading, becomes a more relevant indicator than the static modulus.

Applying the NPA-CCS material dynamic modulus and damping into the project and observing over years of operation, it can be stated that the design was successful. There was no maintenance, not even ballast cleaning required on either project, with the expected number of vehicles passes matching the design expectations. Figure 16a and Figure 16b show that for the Pasqua loop, even the inside track did not move at all. Typically, where there is the risk of inside track moving inwards or settling into the ballast, heavier

ties (like concrete ties) are recommended (Chatterjee et al., 2024[29]). However, owing to the high damping effect and minimum loss of material modulus over passes with varying speed, neither expensive concrete ties nor maintenance was necessary. This performance was an exact match to the pre-construction design. The Pasqua loop was surveyed monthly, and the maximum vertical track movement observed was around 6mm within the initial two and a half years (June 2022 to December 2024) of operation. There was no lateral movement, and cross-level issues were observed on the track. Even at the loop turn around and patches where the subgrade CBR (California Bearing Ratio) was less than 2%. There has been no maintenance through the initial two and a half years of observation. No observed ballast fouling or lateral tie movement, or lateral spread ballast from the vibration of the wheels was observed either. Easton, on the other hand, had the stiffness jump from naturally prepared subgrade to concrete. Over the five years of freeze-thaw, it is expected that the natural subgrade will lose some strength. Also, the impact of the stiffness jump was expected to create additional strains within the CCS material. Since the design had accounted for these weakening conditions, it was possible to operate on the track without any maintenance for more than five years (September 2019 to March 2025). This aligns well with the 6.7 times maintenance reduction using NPA-CCS reported by the US Federal Railway Administration (Palese, 2018[33]).

Based on the observations from the two full-scale applied projects, it can be stated that the dynamic elastic modulus and the ratio of the dynamic viscous modulus to the dynamic elastic modulus are vital parameters for calculating the acceptable design life. However, an instrumented study in future would help with calibrating the true in-situ strains with material dynamic properties.

Figure 16a. The operational Pasqua site after 3.5 years

Figure 16b. Pasqua loop in April 2025 (after 3.5 years of operation with no maintenance)

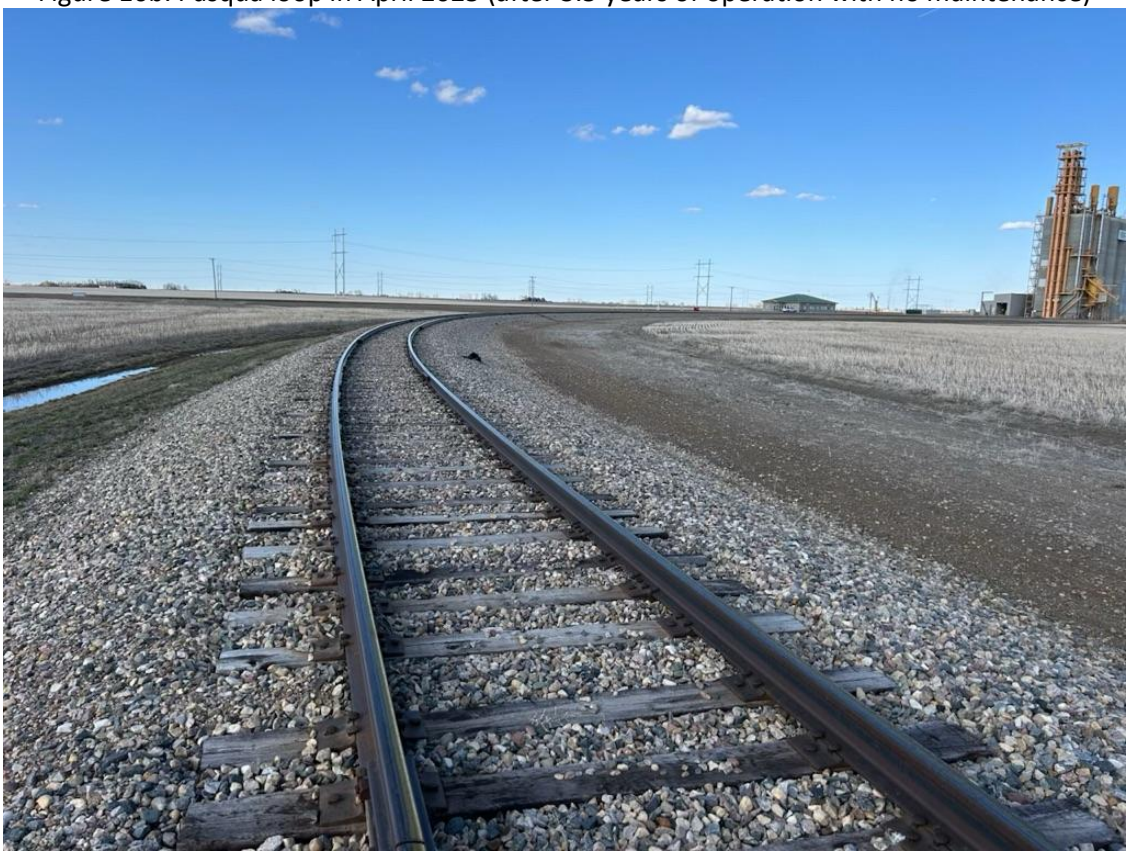

Figure 17. The relationship between phase angle and allowable passes with Dynamic Elastic Modulus

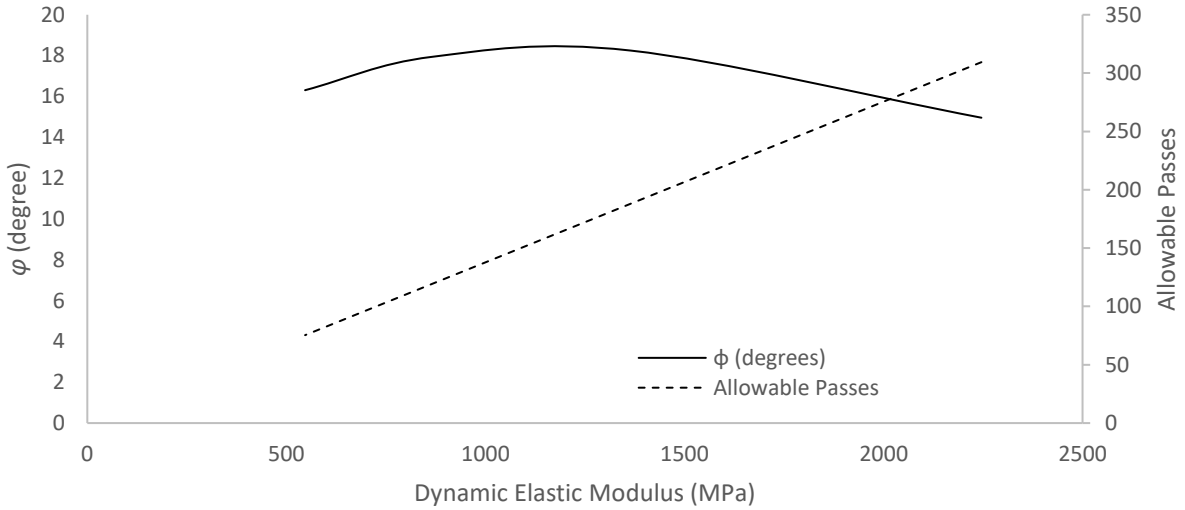

Figure 18. Understanding the allowable passes based on in-situ forces and CCS dynamic elastic modulus

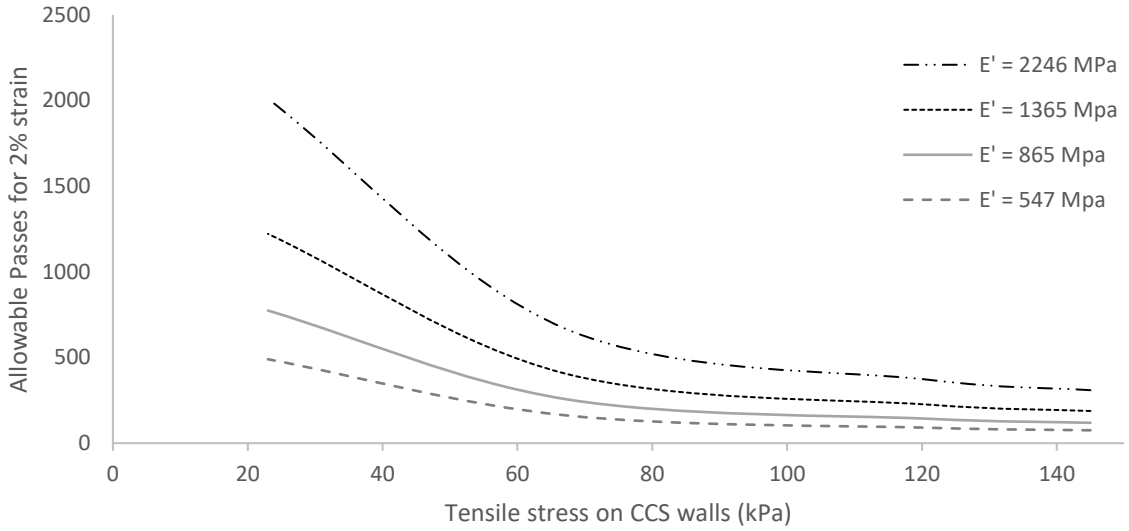

Conclusion

The current paper introduces the importance of considering the dynamic modulus of geocell (CCS) in designing railway embankments. CCS being a viscoelastic material, it is not just the static maximum load, but consideration for the progressive strain accumulation with every passing load is crucial for design. Understanding and utilizing dynamic material properties such as modulus and strain accumulation rate are essential for optimizing the design and long-term performance of CCS-stabilized rail embankments. This study contributes to the development of a more robust, performance-based design methodology for geocell applications in railway engineering. The design was implemented with success over two full-scale projects in Saskatchewan, Canada. Results show the huge potential of utilizing the damping and modulus of high-strength reinforcing geocell materials like NPA-geocell in developing rail infrastructure.

References

[1] Nimbalkar S., Piyush Punetha P., Kaewunruen S. Performance Improvement of Ballasted Railway Tracks Using Geocells: Present State of the Art. Part of the Springer Transactions in Civil and Environmental Engineering book series (STICEE). doi: 10.1007/978-981-15-6095-8_11. (2020)

[2] Pokharel S.K., Breault M. (2020). High-strength polymeric geocell-reinforced railway line repair in degraded permafrost conditions. Industrial Fabrics Association International (IFAI / ATA) Conference.

[3] Pokharel, S. K. Experimental Study on Geocell-Reinforced Bases under Static and Dynamic Loading. Civil, Environmental, and Architectural Engineering Department, University of Kansas, Kansas, USA. (2010)

[4] Chatterjee A., Pokharel S.K., Breault M. (2023). Polymeric Alloy Geocell Reinforced Design for a Heavily Loaded Gravel Pad with Restricted Fill Thickness. Industrial Fabrics Association International (IFAI / ATA), Kansas City, USA.

[5] Hegde, A., Hasthi, Venkateswarlu. (2018). Numerical Analysis of Machine Foundation Resting on the Geocell Reinforced Soil Beds. Geotechnical Engineering. 49. pp 55-62.

[6] Mehrjardi Gh. Tavakoli, S.N. Moghaddas Tafreshi, A.R. Dawson. (2012) Influence of Geocell reinforcement on damping properties of the trench with pipe. 15th European Conference on Soil Mechanics and Geotechnical Engineering. pp1073

[7] Chatterjee A. K., Schary Y., Pokharel S. K., "Structural Contribution of Dynamic Modulus of Cellular Confinement System in Pavement Stabilization". Proceedings of Geotechnical Frontiers 2025. 365-375 doi:10.1061/9780784485972.036.

[8] Chatterjee A., Pokharel S., Breault M. 2024. Rehabilitation Design of Railway Tracks Using High-Strength Polymeric Geocell. ASCE. Geo-Congress 2024 GSP 350. pp 467-475. doi.org/10.1061/9780784485323

[9] Chatterjee A., Pokharel S., Breault M., Efficacy of geocell modulus in reducing dynamic load factor on railway track subjected to freeze-thaw. Proceedings of the Second Canadian & Cold Region Rail Research Conference 2024. Edmonton. April 2024. 155-162.

[10] Dagenais T.L., Chatterjee A.K., Pokharel S.K., Breault M., Approaching road design from a sustainability perspective. Proceedings of GeoShanghai 2024. May 2024. Shanghai, China.

[11] Chatterjee A., Dagenais T., Pokharel S., Breault M., Simplified Model for Road Sustainability Evaluation. Canadian Society of Civil Engineers Conference 2024. June 2024. Niagara, Canada.

[12] Amiri A., Moghaddas Tafreshi S.N., Dawson A.R. (2023). Vibration response of machine foundations protected by the use of adjacent multi-layer geocells. Journal of Geotextiles and Geomembranes. ISSN 0266-1144.

[13] Camila B. S. de Alvarenga, Effect of an Embankment Reconstruction Using a Wicking Geotextile in the Drainage and Strength of Subgrade. Master of Science in Geotechnical Engineering, Department of Civil and Environmental Engineering, University of Alberta (2021).

[14] Indraratna B, Biabani MM, Nimbalkar S (2015) Behaviour of geocell-reinforced sub-ballast subjected to cyclic loading in plane-strain conditions. Journal of Geotech Geoenvironmental Engineering 141(1):04014081

[15] Nimbalkar, S., Indraratna, B., Dash, S.K., Christie, D. Improved Performance of Railway Ballast under Impact Loads Using Shock Mats. Journal of Geotechnical and Geo-environmental Engineering 138(3), 281-294 (2012)

[16] Kief O., Rajagopal K., Veeraragavan A., Chandramouli S. (2011) Modulus improvement factor for geocell-reinforced bases. Geosynthetics India. 2011 Sep-11

[17] Leshchinsky, B., Ling, H.I. Numerical modelling of behaviour of railway ballasted structure with geocell confinement. Geotextiles and Geomembranes 36, 33-43 (2013).

[18] Mehrjardi G.T., Motarjemi F., Interfacial properties of geocell-reinforced granular soils. Geotextiles and Geomembranes.46(4). 2018. 384-395. ISSN 0266-1144. doi.org/10.1016/j.geotexmem.2018.03.002.

[19] Dunn L. (2019). Introduction to Viscoelasticity in Polymers and its Impact on Rolling Resistance in Pneumatic Tyres. International Journal of Squiggly and Wobbly Materials, v23(1)

[20] Findley, W.N.; Lai, J.S.; Onaran, K.; Christensen, R.M. Creep and Relaxation of Nonlinear Viscoelastic Materials with an Introduction to Linear Viscoelasticity; Dover Publications: New York, NY, USA, 1977.

[21] Wineman A., Nonlinear viscoelastic solids—A review. Math. Mech. Solids 2009, 14, 300–366

[22] Banks, H.T., Hu,S., Kenz, Z.R.; A brief review of elasticity and viscoelasticity for solids. Adv. Appl. Math. Mech. 2011, 3, 1–51

[23] Lin CY, Chen YC, Lin CH, Chang KV. "Constitutive Equations for Analyzing Stress Relaxation and Creep of Viscoelastic Materials Based on Standard Linear Solid Model Derived with Finite Loading Rate." Polymers (Basel). 2022 May 23;14(10):2124. doi: 10.3390/polym14102124. PMID: 35632006; PMCID: PMC9143375.

[24] Lakes R.S. "Viscoelastic Materials." *Cambridge University Press*; New York, NY, USA: 2009.

[25] Riande E., Diaz-Calleja R., Prolongo M., Masegosa R., "Salom C. Polymer Viscoelasticity: Stress and Strain in Practice." *CRC Press*. Boca Raton, FL, USA: 1999.

[26] Manual for Railway Engineering. AREMA (American Railway Engineering and Maintenance-of-Way Association). 2019

[27] Emersleben, Ansgar & Meyer, Nathália. (2009). 'Interaction between hoop stresses and passive earth resistance in single and multiple geocell structure'. Proc., GeoAfrica: 1st African Regional Conf. on Geosynthetics. 1-10

[28] ISO/TD 18228-5:2025. Design using geosynthetics. Part 5: Stabilization. First edition 2025-01

[29] Chatterjee A., Pokharel S., Breault M., "Rehabilitation of rail track facing cross-level issues using polymeric geocell." Proceedings of the GeoAmericas 2024. 5th Pan-American Conference on Geosynthetics. April 28 - May 1, 2024. Toronto, Canada

[30] Mohagheghian, Iman & McShane, Graham & Stronge, W.J. (2015). Impact perforation of monolithic polyethylene plates: Projectile nose shape dependence. International Journal of Impact Engineering. 80. 10.1016/j.ijimpeng.2015.02.002

[31] ASTM D8269-21. Standard Guide for the Use of Geocells in Geotechnical and Roadway Projects

[32] ASTM D7361-07. Standard Test Method for Accelerated Compressive Creep of Geosynthetic Materials Based on Time-Temperature Superposition Using Stepped Isothermal Method.

[33] Palese J., Hartsbough C.M., Zarembski A.M., Ling H.I. Field Demonstration of Geocell Track Substructure Support System Under High-Speed Passenger Railroad Operations. U.S. Department of Transportation Federal Railroad Administration Office of Railroad Policy and Development. July 2018.